

This article was downloaded by:

On: 25 January 2011

Access details: *Access Details: Free Access*

Publisher *Taylor & Francis*

Informa Ltd Registered in England and Wales Registered Number: 1072954 Registered office: Mortimer House, 37-41 Mortimer Street, London W1T 3JH, UK



Separation Science and Technology

Publication details, including instructions for authors and subscription information:

<http://www.informaworld.com/smpp/title~content=t713708471>

Solute Separation by Continuous Bubble Fractionation

B. T. Kown^a; L. K. Wang^a

^a COLLEGE OF ENGINEERING RUTGERS UNIVERSITY, NEW JERSEY

To cite this Article Kown, B. T. and Wang, L. K. (1971) 'Solute Separation by Continuous Bubble Fractionation', *Separation Science and Technology*, 6: 4, 537 — 552

To link to this Article: DOI: 10.1080/00372367108056037

URL: <http://dx.doi.org/10.1080/00372367108056037>

PLEASE SCROLL DOWN FOR ARTICLE

Full terms and conditions of use: <http://www.informaworld.com/terms-and-conditions-of-access.pdf>

This article may be used for research, teaching and private study purposes. Any substantial or systematic reproduction, re-distribution, re-selling, loan or sub-licensing, systematic supply or distribution in any form to anyone is expressly forbidden.

The publisher does not give any warranty express or implied or make any representation that the contents will be complete or accurate or up to date. The accuracy of any instructions, formulae and drug doses should be independently verified with primary sources. The publisher shall not be liable for any loss, actions, claims, proceedings, demand or costs or damages whatsoever or howsoever caused arising directly or indirectly in connection with or arising out of the use of this material.

Solute Separation by Continuous Bubble Fractionation

B. T. KOWN and L. K. WANG

COLLEGE OF ENGINEERING
RUTGERS UNIVERSITY
NEW BRUNSWICK, NEW JERSEY 08903

Summary

A continuous bubble fractionation system consisting of a vertical Plexiglas tube provided with a source of air bubbles, means of continuous liquid feed, overflow, and bottom effluent has been operated to study the performance of the system. The study primarily involves an examination of the effects of variables such as gas rate, liquid rate, solute concentration, and column size on the effectiveness of the system for separating an organic solute from a dilute aqueous solution.

The experimental results indicate that the effects of gas and liquid rate on the performance have generally followed the results expected from an equilibrium adsorption of a surfactant on the gas-liquid interface described by Gibbs' equation and material balances. An increase in gas rate increased the effectiveness of the system by providing more adsorption surface. The adverse transfer of the solute by the eddy diffusion caused by rising bubbles was found to be the factor limiting the effectiveness of the system.

INTRODUCTION

Bubble fractionation, a separation technique based on adsorption of a solute on the surfaces of gas bubbles rising through a solution and subsequent removal of the concentrated liquid layer from the top, as a possible means of separating the solute was first proposed by Lemlich and Dorman (1). Like foam fractionation, bubble fractionation is based on the phenomenon that a solute of a surface-active nature is adsorbed

on gas-liquid interface. Bubble fractionation differs from foam fractionation in that the former depends on the existence of the concentration gradient in the solution, while the latter is based on the formation of the stable foam phase above the liquid. The performance characteristics of a foam fractionation system is such that its effectiveness is primarily controlled by the parameters of the foam phase rather than those of the liquid phase, and accordingly the investigations in the field to date have been chiefly concerned with the foam phase (2). In the case of a bubble fractionation system, its effectiveness must rely on the existence of the concentration gradient in the solution phase, and an understanding of the parameter governing the concentration gradient in the solution phase is essential for an evaluation of the system.

Lemlich (3) has presented some theoretical considerations for batch-wise fractionation and its qualitative accord with experimental data of a preliminary nature (4). The purpose of this paper is to present the results of an investigation conducted to study the performance of a continuous bubble fractionation system.

PARAMETERS

The solute and over-all material balances around the bottom end of a continuous bubble fractionation column, far below the feed point, such as shown in Fig. 1a, are

$$DA(dC/dy) + (V_b + V_e)C = V_e C_e + V_b C_b + fG\Gamma \quad (1)$$

and in a similar manner the balances above the feed point may be expressed by

$$DA(dC/dy) + V_t C_t = (V_t - V_b)C + V_b C_b + fG\Gamma \quad (2)$$

where the terms on the left of Eq. (1) represent the solute entering the envelope by the axial diffusion and the downflow, while the terms on the right represent the solutes carried out of the envelope by the bottom effluent, the liquid encapsulating the bubbles, and the bubble surfaces.

To obtain a rigorous solution for either Eq. (1) or (2), the exact mechanisms of the solute transfer from the bulk solution to the liquid, i.e., a relationship between C and C_b , and subsequent transfer from the liquid to the bubble surface, i.e., a relationship between C and Γ , must be known. Furthermore, knowledge of the nature and magnitude of the encapsulating liquid, in addition to knowledge on the solute transfer by

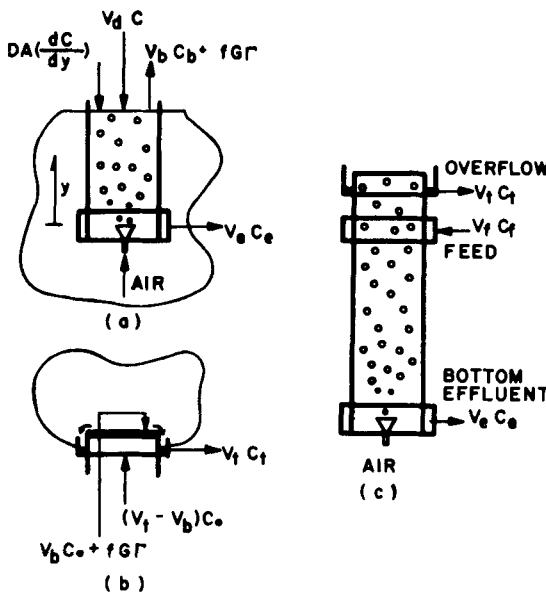


FIG. 1. Solute balances: (a) bottom end, (b) overflow region, and (c) over-all column.

the eddy diffusion, is essential for solving the equation. An attempt to correlate every step of the solute transfer and obtain a rigorous solution for either Eq. (1) or (2) would involve numerous uncertain parameters, and results in the final solution would be so unwieldy that it would be impossible to obtain meaningful information from them.

The probable effects of certain variables on the performance of the separation system may be examined qualitatively by using a solution obtained from either Eq. (1) or (2) with certain approximations. First, when the concentration of the encapsulating liquid (C_b) is assumed to be the same as that of the bulk solution (C), and the bubbles are assumed to be of spherical shape of a uniform size, Eqs. (1) and (2) reduce to

$$DA(dC/dy) + V_e C = V_e C_e + (6/d)G\Gamma \quad (3)$$

and

$$DA(dC/dy) + V_t C_t = V_t C + (6/d)G\Gamma \quad (4)$$

Under equilibrium conditions, solute adsorption at a gas-liquid inter-

face is given by Gibbs' equation:

$$d\gamma = -RT \sum_i \Gamma_i d \ln a_i \quad (5)$$

For a dilute solution of a pure univalent ionic surfactant, Eq. (5) may be written as

$$\Gamma = - (C/2RT) (d\gamma/dC) \quad (6)$$

In the case of foam fractionation, the surface excess in the foam phase is often found to be constant and independent of the concentration, representing the saturated interface condition. However, in the case of bubble fractionation the foam phase is not produced, and the bubble surface may not be saturated. It may be approximated that for a low concentration, the variation of the surface excess with respect to the concentration is represented by the linear relationship

$$\Gamma = \alpha C \quad (7)$$

and at a high concentration, the surface excess levels off to a constant value, representing the complete saturation of the bubble surface. With the linear relationship between the surface excess and solute concentration, the concentration profile in the column below the feed point is expressed by

$$\begin{aligned} \frac{C}{C_e} &= \frac{(6/d)\alpha G}{(6/d)\alpha G - V_e} \exp \left\{ \frac{(6/d)\alpha G - V_e}{DA} y \right\} - \frac{V_e}{(6/d)\alpha G - V_e} \\ &\cong 1 + \frac{(6/d)\alpha G}{DA} y + \frac{1}{2} \frac{(6/d)\alpha G}{DA} \frac{(6/d)\alpha G - V_e}{DA} y^2 + \dots \end{aligned} \quad (8)$$

and in the case of a batchwise operation, the concentration profile in the column is

$$\begin{aligned} \frac{C}{C_e} &= \exp \left\{ \frac{(6/d)\alpha G}{DA} y \right\} \\ &\cong 1 + \frac{(6/d)\alpha G}{DA} y + \frac{1}{2} \left[\frac{(6/d)\alpha G}{DA} \right]^2 y^2 + \dots \end{aligned} \quad (9)$$

If a constant value of the surface excess is assumed, Eqs. (8) and (9)

become

$$C = C_e + \frac{(6/d)\beta G}{V_e} \left[1 - \exp \left\{ \frac{V_e}{DA} y \right\} \right] \quad (10)$$

and

$$C = C_e + \frac{(6/d)\beta G}{DA} y \quad (11)$$

Equations (9) and (11) are essentially the same as Lemlich's Eqs. (14) and (16) (2).

No attempts were made in this investigation to evaluate the parameters shown in Eqs. (8), (9), (10), and (11). A bubble fractionation system was operated both in continuous and batch modes using gas rates, liquid rates, solute concentrations, and column sizes as variables in order to obtain general information on the effects of these variables on the performance. Equations (1) and (2), which do not include the feed, are not expected to describe the column performance accurately, even if the assumptions were to be correct. These equations and their solutions are used only to have a qualitative comparison with the experimental results.

EXPERIMENTAL APPARATUS & MATERIAL

Four bubble fractionation columns made of 6-ft Plexiglas tubes of different diameters (2.54, 3.18, 6.35, 12.70 cm) were used for the study. Each column had provision for overflow, feed, and bottom effluent. The liquid in the column was allowed to flow over the top, while sets of four equally spaced holes were used for the feed and the bottom effluent. The columns were provided with several sampling holes of hypodermic needle size along the vertical length. A schematic diagram of the apparatus is shown in Fig. 2.

Thoroughly humidified air was introduced through a sintered glass diffuser placed near the bottom. The rotameters, in combination with timed volumetric measurements of the liquid flow, were used for the overflow, feed, and gas rate measurement. The average bubble size was estimated from photographs of the bubbles made near the top and bottom of the column. All experiments were conducted at room temperature.

An aqueous solution of crystal violet chloride (hexamethylpararo-

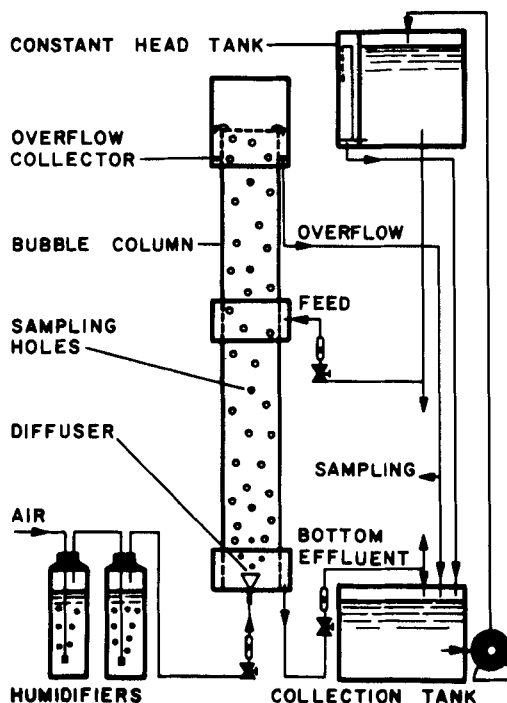


FIG. 2. Schematic diagram of the continuous bubble fractionation system.

saniline chloride) was used for the study. Selection of crystal violet chloride dye was based on the simplicity of the concentration determination and the convenience of the visual observation of the concentration profile during operation. The samples from the column were taken after 30 min of operation, a time found to be sufficient for a steady-state in both the continuous and batch operations with the gas rate in the range used in this investigation. The solute concentration in the samples were determined by a photoelectric colorimeter. A material balance made on the input vs. the output indicates that loss of solute due to adsorption on the system and possible decomposition during a test was insignificant. The variation of the surface tension with respect to the solute concentration was determined by the "Capillary Tube Method," and the results are shown in Fig. 10. By using Eq. (6), the surface excess (0.396×10^{-10} g-mole/cm²) was estimated from the surface tension measurement.

RESULTS AND DISCUSSION

The effects of the column diameter on the solute transfer were examined with the columns of four different sizes operated under the same condition; 9.16 CCS of the gas rate, 1.67 CCS of the feed, 1.28 CCS of the bottom effluent, and 2.25×10^{-8} g-mole/cm³ of the feed concentration. The experimental results are shown in Fig. 3 in which the concentration profiles are plotted on semilogarithmic coordinates. The solute concentration of the overflow and feed are also shown in Fig. 3. The solute concentration at the top of the column was measured 1.0 cm below the liquid surface. The same four columns were also operated as a batch system with 5.0 CCS of the gas rate and 2.25×10^{-8} g-mole/cm³ of the initial feed concentration. The results of the batch study are shown in Fig. 4.

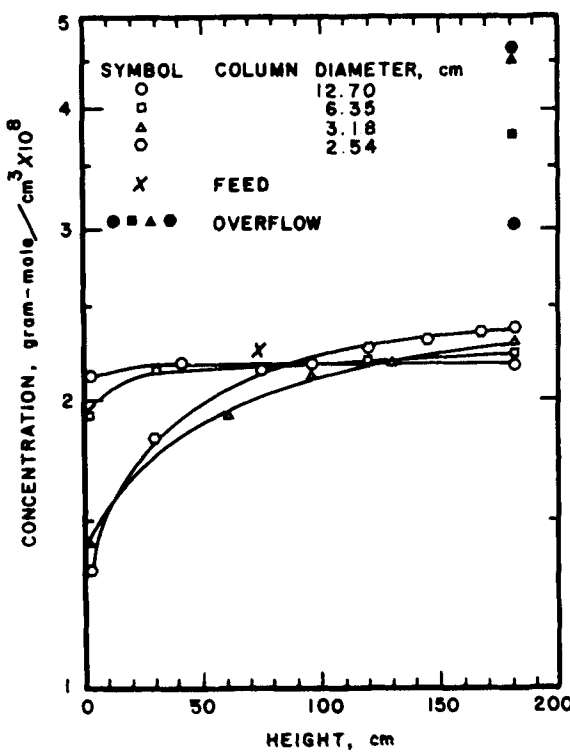


FIG. 3. Effect of diameter on concentration profile of continuous column.

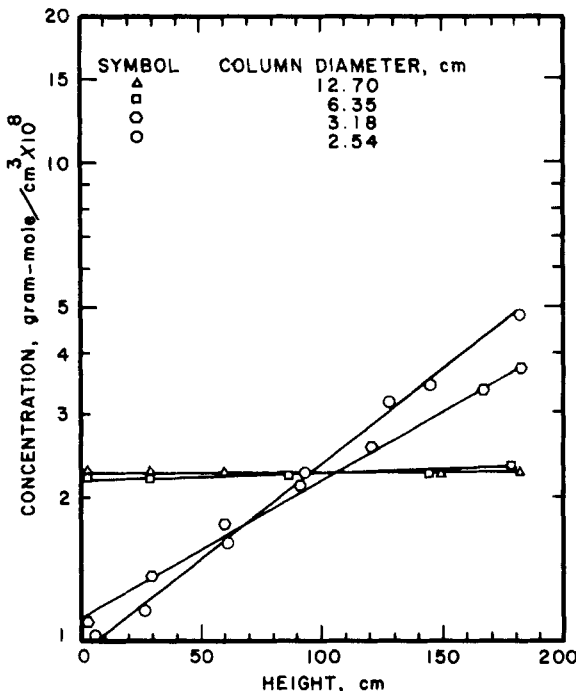


FIG. 4. Effect of diameter on concentration profile of batch column.

The concentration profiles shown in Figs. 3 and 4, even though numerical accord was not obtained, are in general agreement with a pattern described by Eqs. (8) and (9), or Eqs. (10) and (11). Equation (3) suggests that near the bottom, the concentration gradient decreases as the cross section increases. In addition, it has been shown that the diffusion coefficient (D) also increases as the column diameter increases (5), and this also contributes to the diminishing concentration gradient in a larger column. It is quite evident in the experimental results that an increase in the column diameter greatly increases the axial mixing, and thereby diminishes the concentration gradient in the column.

The nearly constant slope of each profile shown in Fig. 4 may seem to indicate that the profile is expressed by an exponential form (Eq. 9), and hence the solute adsorption on the bubble surface is linearly proportion to the concentration (Eq. 7). However, further examination of the results indicated that the experimental data are insufficient to con-

clude the exact nature of the solute adsorption. The plot of the same data on linear coordinates also produced straight lines from the bottom to near the top, curving up only in a small upper region. Such a pattern may be interpreted as indicating the surface excess is constant and represents the saturated bubble surface, and that at the top the axial mixing is reduced because of the absence of bubbles above the liquid surface.

The effects of the gas rate on the solute transfer were examined with a 3.18-cm column operated as a batch system with 2.25×10^{-8} g-mole/cm³ of the initial feed, and with the gas rate varying from 1.67 to 20.0 CCS. The same column was also operated as a continuous system with the gas rate varying from 0.75 to 13.3 CCS, while the remaining variables were kept constant for all experiments at 1.67 CCS of the feed, 0.384 CCS of the overflow, and 2.25×10^{-8} g-mole/cm³ of the feed concentration. The results of the batch and continuous operations are shown in Figs. 5 and 6, respectively. In both Figs. 5 and 6, the concen-

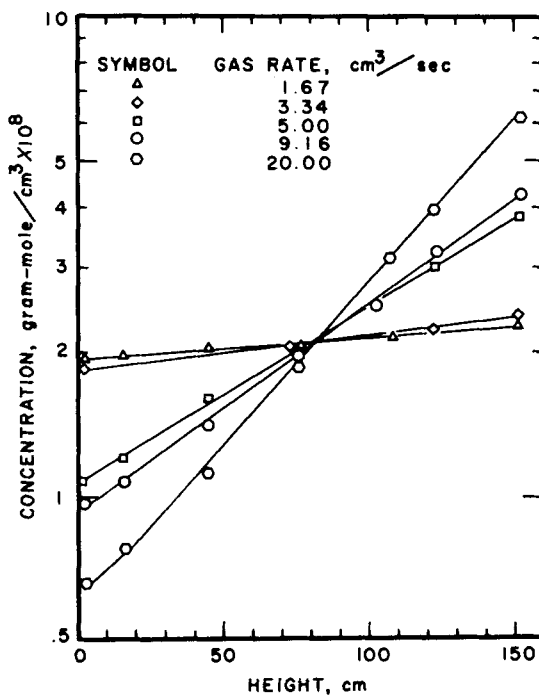


FIG. 5. Effect of gas rate on concentration profile of batch column.

tration profiles for the various gas rates are plotted on semilogarithmic coordinates.

According to Eq. (9), when the concentration profiles in a batch column operated with various gas rates were plotted on semilogarithmic coordinates, the slope of the line for each gas rate would increase linearly with increasing gas rate, assuming the diffusion coefficient is a constant. The results shown in Fig. 5 shows a general tendency for increasing concentration gradient at a higher gas rate; however, the variation of the gradient with respect to the gas rate is somewhat less than that expected from Eq. (9). The discrepancy, i.e., the gradient $d \ln C/dy$ being somewhat less than a linear function of the gas rate, may have resulted from the fact that as the gas rate increases in the actual situation, it not only increases the bubble frequency but also increases the bubble size, the liquid encapsulating the bubble, and the eddy diffusion coefficient (5). The results of the continuous operation shown in Fig. 6

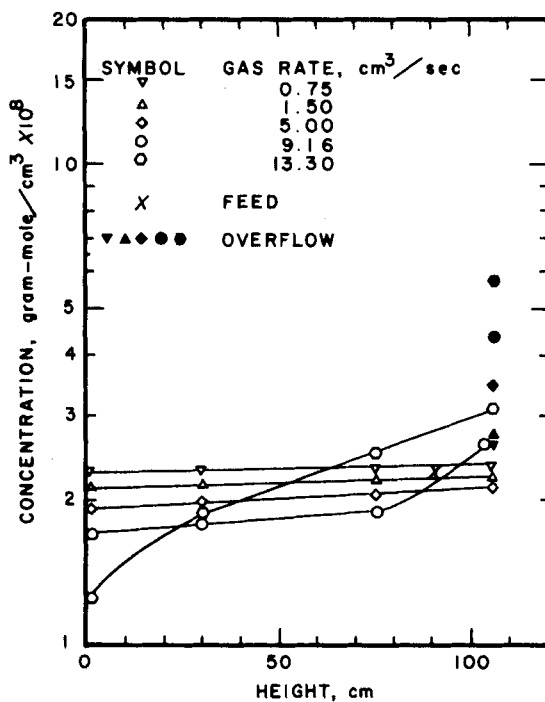


FIG. 6. Effect of gas rate on concentration profile of continuous column.

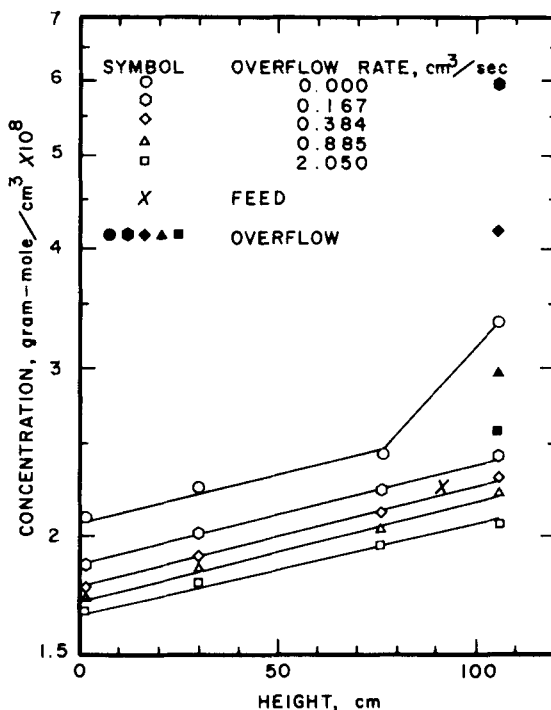


FIG. 7. Effect of overflow on concentration profile of continuous column.

are in general accord with a pattern described by Eq. (8); i.e., near the bottom the concentration gradient increases as the gas rate increases.

The effects of the overflow and the bottom effluent on the concentration profile of a continuous column were also investigated, using 3.18 cm column. Figure 7 shows the profiles in the continuous column operated with the overflow rate varying from 0 to 2.05 CCS while the remaining variables were kept constant at 5.0 CCS of the gas rate, 1.28 CCS of the bottom effluent, and 2.25×10^{-8} g-mole/cm³ of the feed concentration. In a similar manner, Fig. 8 shows the results of the continuous operation with the bottom effluent varying from 0.82 to 2.50 CCS, while the gas rate, overflow, and feed concentration were kept constant for all experiments; 9.16 CCS, 1.25 CCS, and 2.25×10^{-8} g-mole/cm³, respectively. The general pattern of the curves shown in Figs. 7 and 8 are expected from Eq. (8).

Description of the solute transfer and its balance around the overflow

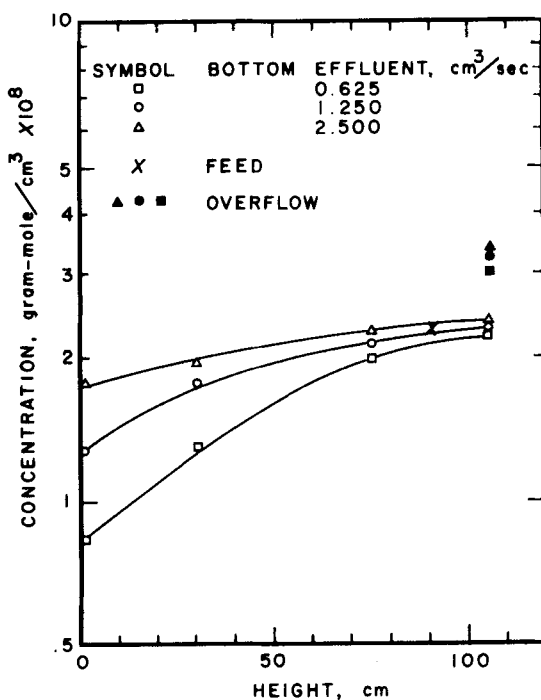


FIG. 8. Effect of bottom effluent on concentration profile of continuous column.

region, shown in Fig. 1b, is complicated by the fact that a bubble breaks above the liquid surface and the liquid phase no longer exists. It is doubtful whether the same diffusion coefficient value would apply for a point very near the liquid surface and a point far away from the surface. Furthermore, when a bubble breaks, a part of the liquid is collected directly into the overflow, while the remaining liquid falls back into the bulk solution. The distribution of the liquid from a bursting bubble depends on a number of variables including the column size. Because the overflow was taken over the side of the column rather than throughout the cross section, the flow near the surface is no longer one-dimensional. It is debatable whether the solute concentration in the overflow (C_t) should be the same as that (C_o) of the bulk solution near the top.

When the bulk solution is nearly homogeneous near the top, i.e., when the concentration profile is flat near the top, the eddy diffusion term of

Eq. (4) become insignificant, and Eq. (4) reduces to

$$V_t C_t = V_t C_o + (6/d) G \Gamma \quad (12)$$

where C_o is the solute concentration at the top. The same result would be obtained if the diffusion coefficient (D) was insignificant in this region. It may be noted here that Eq. (12) is the result of the assumption that the solute concentration in the encapsulating liquid (C_b) is the same as that (C_o) of the bulk solution near the top. Equation (12) is similar to that commonly used for foam fractionation, derived from the so-called "ideal foam model" (6, 7) in which the complete removal of the liquid from the bursting bubbles is assumed.

In every test of continuous operation, the solute concentration in the overflow was significantly higher than that measured 1.0 cm below the liquid surface, which suggests that Eq. (2) may be inadequate for the description of the material balance in the overflow region.

An effort was made to compare the experimental result obtained from the gas rate study, shown in Fig. 6, with Eq. (12). When the surface excess is a linear function of the solute concentration (Eq. 7), Eq. (12)

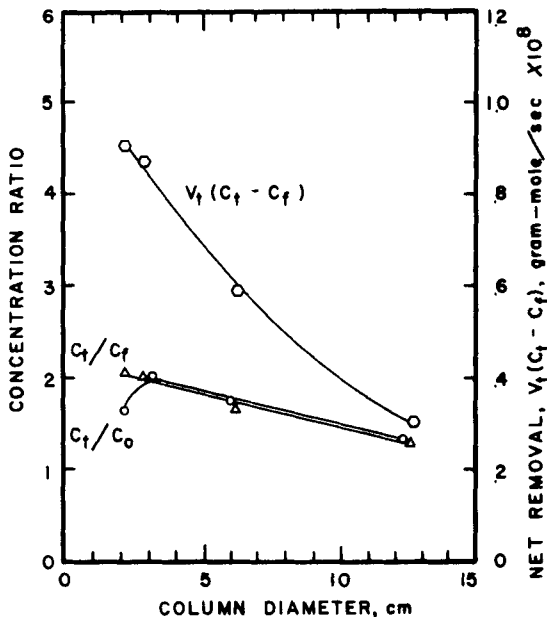


FIG. 9. Effect of gas rate on solute separation.

is reduced to

$$\frac{C_t}{C_o} = 1 + [(6/d) \alpha G / V_t] \quad (13)$$

The net removal, $V_t(C_t - C_f)$, and the concentration ratios, C_t/C_o and C_t/C_f , as a function of the gas rate are shown in Fig. 9.

The experimental value of the surface excess was estimated using Eq. (12) and bubble diameters estimated from the photographs. The value varied in a wide range with the maximum value of 0.232×10^{-10} g-mole/cm² for the smallest column operation, shown in Fig. 3.

The experimental results shown in Fig. 9 generally followed the patterns described by Eqs. (12) and (13). However, it is not the investigator's intention to imply that these equations describe bubble fractionation accurately. The equations are used only to emphasize the fact that the solute concentration of the overflow is significantly higher than that of the bulk solution, and under certain circumstances the performance of a bubble fractionation system is very similar to that of a foam fractionation system, especially when most of the liquid from the bursting bubbles above the surface is collected into the overflow.

Despite our efforts, the experimental findings of this study were insufficient to clarify certain questions, especially ones concerning the

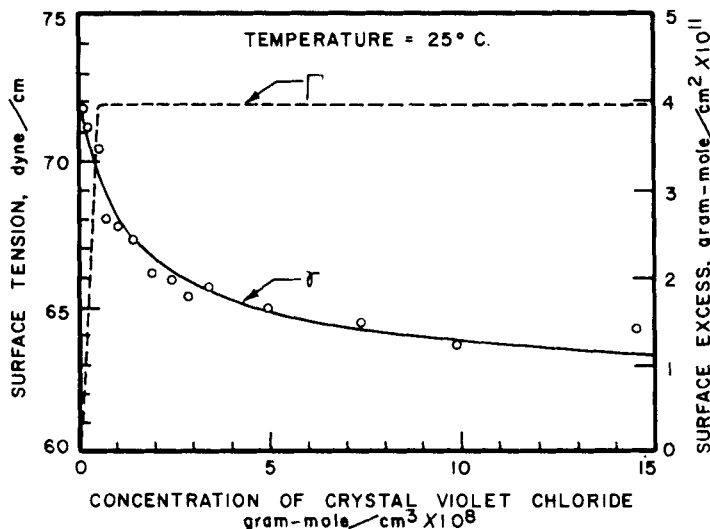


FIG. 10. Surface tension measurement of Crystal Violet Chloride solution.

fundamental mechanism of the adsorption process and subsequent transfer through the column to the top and over the column. Further investigations of bubble fractionation using different solutions and varying column heights would be needed to reach a better understanding of the fundamental mechanism involved.

CONCLUSION

The continuous bubble fractionation process was initially investigated with the hope that under proper operating conditions, the rising bubbles, enriched with the solute, would create a concentration gradient so steep that removal of a small fraction of the feed from the top would result in an effective separation of the solute. However, it appears that in a practical bubble fractionation system the axial mixing caused by rising bubbles is so intense that unless the liquid from bursting bubbles is immediately and completely removed, the liquid will be redispersed back into the bulk solution, thereby losing the effectiveness of the system.

When an extremely small column with sufficient overflow is used, most of the solute adsorbed on the bubble surfaces is removed. For a realistic column size, the intensive axial mixing causes the bulk solution in the column to be more or less homogeneous throughout the column. A large column would be ineffective in solute separation unless some means of collecting the liquid from bursting bubbles is provided to prevent the liquid from redispersing back into the bulk solution.

When a small column is operated with sufficient overflow, the solute removed with the overflow generally increased as the gas rate and feed concentration were increased. The increase in the adsorption for a high solute concentration is due chiefly to an increase in the adsorption surface which results from the smaller size bubbles generated in the concentrated solution.

Notation

a = solute activity

A = column cross section, cm^2

C = solute concentration, $\text{g-mole}/\text{cm}^3$

d_c = column diameter, cm

d = bubble diameter, cm

D = axial diffusion coefficient, cm^2/sec

f = surface to volume ratio of bubble, cm^2/cm^3

G = volume rate of gas, cm^3/sec (CCS)

V = volume rate of liquid, cm^3/sec (CCS)

y = height of column from bottom, cm

Greek Letters

α = equilibrium constant of surface adsorption, cm^3/cm^2

β = saturated surface concentration, g-mole/ cm^2

γ = surface tension, dyne/cm

Γ = surface excess, g-mole/ cm^2

Subscripts

b = liquid encapsulating bubble

e = bottom effluent

f = feed

o = solution immediately below the liquid surface

t = overflow

Acknowledgment

The work upon which this publication is based was supported by a research grant from the Office of Water Resource Research, U.S. Department of the Interior.

REFERENCES

1. D. C. Dorman and R. Lemlich, "Separation of Liquid Mixture by Non-Foaming Bubble Fractionation," *Nature*, **207**(4993), 145-146 (July 1965).
2. R. Lemlich, "Adsorptive Bubble Separation Methods," *Ind. Eng. Chem.*, **60**(10), 16-29 (1968).
3. R. Lemlich, "Theoretical Approach to Nonfoaming Adsorptive Bubble Fractionation," *A.I.Ch.E. J.*, **12**(4), 802-804 (July 1966).
4. D. O. Harper and R. Lemlich, "Direct Visual Observation of Nonfoaming Adsorptive Bubble Fractionation," *A.I.Ch.E. J.*, **12**(6), 1220-1221 (November 1966).
5. T. Reith, S. Renken, and B. A. Israel, "Gas Holdup and Axial Mixing in the Fluid Phase of Bubble Column," *Chem. Eng. Sci.*, **23**(6), 619-629 (1968).
6. I. H. Newson, "Foam Separation: The Principle Governing Surfactant Transfer in a Continuous Foam Column," *J. Appl. Chem.*, **16**, 43-49 (1966).
7. R. K. Wood and T. Tran, "Surface Adsorption and the Effects of Column Diameter in the Continuous Foam Separation Process," *Can. J. Chem. Eng.*, **44**, 322-326 (1966).

Received by editor September 10, 1970